Transition to long-range magnetic order in the highly frustrated insulating pyrochlore antiferromagnet Gd$_2$Ti$_2$O$_7$

N. P. Raju*

Brockhouse Institute for Materials Research and Department of Chemistry, McMaster University, Hamilton, Ontario, Canada L8S 4M1

M. Dion[†]

Department of Physics, University of Waterloo, Waterloo, Ontario, Canada N2L 3G1

M. J. P. Gingras[‡]

Laboratoire Louis Néel, Centre National de la Recherche Scientifique, Boîte Postale 166, 38042, Grenoble, Cedex, France

T. E. Mason[§]

Department of Physics, University of Toronto, Toronto, Ontario, Canada M5S 1A7

J. E. Greedan

Brockhouse Institute for Materials Research and Department of Chemistry, McMaster University, Hamilton, Ontario, Canada L8S 4M1

(Received 2 December 1998)

Experimental evidence from measurements of the ac and dc susceptibility, and heat-capacity data show that the pyrochlore structure oxide, Gd$_2$Ti$_2$O$_7$, exhibits short-range order that starts developing at 30 K, as well as long-range magnetic order at $T \sim 1$ K. The Curie-Weiss temperature, $\theta_{CW} = -9.6$ K, is largely due to exchange interactions. Deviations from the Curie-Weiss law occur below ~ 10 K while magnetic heat-capacity contributions are found at temperatures above 20 K. A sharp maximum in the heat capacity at $T_c = 0.97$ K signals a transition to a long-range-ordered state, with the magnetic specific accounting for only $\sim 50\%$ of the magnetic entropy. The heat capacity above the phase transition can be modeled by assuming that a distribution of random fields acts on the $^8S_{7/2}$ ground state for Gd^{3+}. There is no frequency dependence to the ac susceptibility in either the short-range- or long-range-ordered regimes, hence suggesting the absence of any spin-glass behavior. Mean-field theoretical calculations show that *no* long-range-ordered ground state exists for the conditions of nearest-neighbor antiferromagnetic exchange *and* long-range dipolar couplings. At the mean-field level, long-range order at various commensurate or incommensurate wave vectors is found only upon inclusion of exchange interactions beyond nearest-neighbor exchange and dipolar coupling. The properties of Gd$_2$Ti$_2$O$_7$ are compared with other geometrically frustrated antiferromagnets such as the Gd$_3$Ga$_5$O$_{12}$ gadolinium gallium garnet, R_2Ti$_2$O$_7$ pyrochlores where R = Tb, Ho, and Tm, and Heisenberg-type pyrochlore such as Y$_2$Mo$_2$O$_7$, Tb$_2$Mo$_2$O$_7$, and spinels such as ZnFe$_2$O$_4$. [S0163-1829(99)03321-4]

I. INTRODUCTION

There has been in the past eight years an enormous amount of theoretical and experimental activity devoted to the study of highly geometrically frustrated antiferromagnetic materials.[1] The main reason for this interest stems from the suggestion that a high degree of frustration can induce sufficiently large zero-temperature quantum spin fluctuations as to destroy long-range Néel order even in three dimensions. This could give rise to new exotic and intrinsically quantum-mechanical magnetic ground states such as dimerized ground states, ''spin nematics,'' or fully disordered states (e.g., resonating-valence-bond-like) with no broken spin or lattice symmetries.[2–4] Frustration arises when a magnetic system cannot minimize its total classical ground-state energy by minimizing the bond energy of each spin-spin interaction individually.[5] This is the case, for example, in systems where antiferromagnetically coupled spins reside on a network made of basic units such as triangles or tetrahedra. On a triangular plaquette, vector (i.e., XY or Heisenberg) spins can manage the frustration better than Ising moments

by adopting a noncollinear structure with the spins making an angle of 120° from each other. Triangular or tetrahedral units can be put together to form a regular lattice such that they are either *edge sharing* or *corner sharing*. For example, the space-filling arrangements of edge-sharing triangles and tetrahedra form the well-known triangular and face-centered-cubic lattices in two and three dimensions, respectively. In two dimensions, a network of corner-sharing triangles forms the kagomé lattice.[1–3] In three dimensions, a lattice of corner-sharing tetrahedra forms the structures found in spinels, Lave phases, and pyrochlore crystals,[4,6,7] while corner-sharing triangles give the familiar garnets.[8–12]

Among highly frustrated antiferromagnets, the three-dimensional pyrochlore lattice of corner-sharing tetrahedra is a particularly interesting system (see Fig. 1). Theory[7,13,14] and Monte Carlo simulations[14,15] show that classical Heisenberg spins residing on the vertices of the pyrochlore lattice and interacting only via nearest-neighbor antiferromagnetic exchange do not show a transition to long-range magnetic order at nonzero temperature. This is very different from the also frustrated classical nearest-neighbor fcc Heisenberg an-
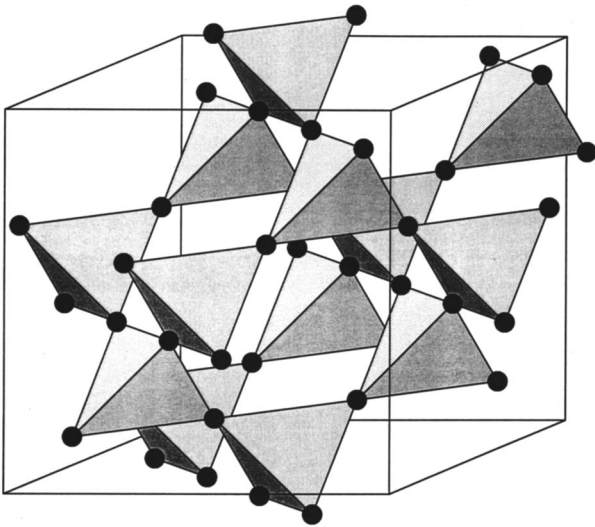
FIG. 1. Pyrochlore lattice of corner-sharing tetrahedra.

tiferromagnet where long-range order occurs at finite temperature via a first-order transition driven by thermally induced order by disorder.[16-18] Because of their failure to order even at the classical level, the high-frustration present in pyrochlore antiferromagnets would appear to make these systems excellent candidates to search for novel three-dimensional quantum-disordered magnetic ground states. Indeed, recent numerical calculations suggest that the quantum $S=1/2$ pyrochlore Heisenberg antiferromagnet may be a quantum spin liquid.[4]

In all real systems there exist perturbations $\{H'\}$ beyond the nearest-neighbor Heisenberg Hamiltonian such as further than nearest-neighbor exchange, single-ion and exchange anisotropy, and magnetic dipolar couplings. For a classical system, one generally expects that such perturbations will select a unique classical ground state to which a transition at nonzero temperature can occur. It is also possible that the energetic perturbations $\{H'\}$ can sufficiently reduce the classical degeneracy such that "additional" order by disorder via thermal[7,19,20] and/or weak quantum fluctuations,[21] such as occur in the fcc antiferromagnet,[16-18] can "complete" the ground-state selection and give rise to a transition to conventional long-range Néel order at nonzero temperature. However, in the presence of quantum fluctuations (i.e., finite S spin value), one expects that for small spin value S and/or sufficiently weak $\{H'\}$, a quantum-disordered phase may occur.[4,21]

What is perhaps one of the most interesting issues in geometrically frustrated antiferromagnet systems is that a large number of highly frustrated antiferromagnetic insulators exhibit spin-glass behavior rather than spin-liquid behavior. For example, in a number of antiferromagnetic pyrochlore oxides, such as $Y_2Mo_2O_7$ (Refs. 22–24) and $Tb_2Mo_2O_7$,[22,25] spin-glass behavior is observed similar to what is seen in conventional randomly disordered and frustrated spin-glass materials,[26] even though the measured disorder level is immeasurably small in the pyrochlores.[27,28]

Pyrochlores oxides, of which two examples have just been cited, present a number of opportunities for studying geometrically frustrated antiferromagnets. In this structure both cation sites in $Fd\bar{3}m$, the 16c site normally occupied by

a transition element and the 16d site normally occupied by a lanthanide, have the same "pyrochlore" topology, i.e., the three-dimensional network of corner-sharing tetrahedra shown in Fig. 1. Thus materials exist with only the 16c site magnetic $(Y_2Mo_2O_7)$,[22-24] with both sites magnetic $(Tb_2Mo_2O_7)$,[22,25] and with only the 16d site magnetic (the $R_2Ti_2O_7$ materials, for example). This latter series has attracted attention very recently with studies for $R=$ Tm, Ho, and Tb.[29-35] The $R_2Ti_2O_7$ materials are generally quite well-ordered crystallographically, with oxygen nonstoichiometry and 16c/16d site cation admixing at or below the limit of detection by neutron diffraction.[28]

$Gd_2Ti_2O_7$ has not yet been studied in detail and there exist some compelling reasons to do so.[36] Previous reports for $Gd_2Ti_2O_7$ indicate no long-range order down to 1 K.[36] The Gd^{3+} ion $(4f^7)$ is spin only with a $^8S_{7/2}$ ground state and thus, crystal-field splittings and anisotropy, which play a large role in the properties of the aforementioned Tm^{3+}, Ho^{3+}, and Tb^{3+} materials, as will be discussed later, are expected to be relatively unimportant. $Gd_2Ti_2O_7$ then, should be an excellent approximation to a classical Heisenberg antiferromagnetic system with dipole-dipole interactions as leading perturbations $\{H'\}$. In addition it is important to compare this material to the $Gd_3Ga_5O_{12}$, gadolinium gallium garnet (GGG), where the Gd^{3+} ions reside on a three-dimensional sublattice of corner-sharing triangles.[8-12] GGG has been found to possess a very unusual set of thermodynamic properties with anomalous specific-heat behavior, spin-glass magnetic properties, and no true long-range order,[9,10] but incommensurate short-range order developing at very low temperatures.[11] Interesting properties are also observed for applied magnetic fields in the range, 0.1–0.7 T.[12] At the same time Monte Carlo simulations for GGG have found some intrinsic (e.g., disorder-free) glassy behavior with no evidence for the development of short-range order.[9,11] Hence, one further motivation for studying $Gd_2Ti_2O_7$ was to bridge a gap between the peculiar behavior of GGG and the transition-metal pyrochlores, such as $Y_2Mo_2O_7$ and $Tb_2Mo_2O_7$ that show spin-glass behavior and, hence, possibly indirectly gain some insight on the thermodynamic behavior of both GGG and the insulating antiferromagnetic Heisenberg pyrochlore systems.

In this work a detailed study of $Gd_2Ti_2O_7$ has been carried out including both ac and dc susceptibility and heat-capacity studies. To complement the experimental work, results from mean-field theoretical calculations are presented that take into account exchange and dipolar interactions.

II. EXPERIMENTAL METHOD

A. Sample preparation

A polycrystalline sample of $Gd_2Ti_2O_7$ was prepared by high-temperature solid-state reaction. Starting materials Gd_2O_3 and TiO_2 were taken in stoichiometric proportions and mixed thoroughly. The mixture was pressed into pellets and heated in an alumina crucible at 1400 °C in air for 12 h. The powder x-ray diffraction pattern of the sample obtained using a Guinier-Hagg camera indicates that the sample formed is single phase with the cubic pyrochlore structure. The size of the conventional cubic unit cell is $a_0 = 10.184(1)$ Å.

B. dc and ac magnetic susceptibility measurements

The dc magnetic susceptibility χ was measured using a superconducting quantum interference device magnetometer (Quantum Design, San Diego) in the temperature range 2–300 K. The ac susceptibility χ_{ac} was measured at different frequencies by the mutual inductance method. The primary coil of the mutual inductor is energized by a frequency generator (DS 335, Stanford Research Systems) and the output across the two identical secondary coils, wound in opposite directions, was measured using a lock-in amplifier (SR-830 DSP, Stanford Research Systems). The sample susceptibility was determined from the difference in the outputs with the sample in the middle of the top secondary coil and without the sample. The cryostat used for the temperature variation is described in the section below.

C. Specific-heat measurements

The specific heat of the sample in the form of a pellet (≈ 100 mg) was measured in the temperature range 0.6–35 K using a quasiadiabatic calorimeter and a commercial He-liox sorption pumped ^{3}He cryostat supplied by Oxford Instruments. The sample was mounted on a thin sapphire plate with apiezon for better thermal contact. Underneath the sapphire plate a strain gauge heater and a RuO_2 temperature sensor were attached with G-E varnish. The temperature of the calorimetric cell was controlled from the ^{3}He pot on the Heliox. The sample temperature was measured using an LR-700 ac resistance bridge at a frequency of 16 Hz. The specific heat of the sample was obtained by subtracting the contribution of the addendum, measured separately, from the total measured heat capacity.

III. EXPERIMENTAL RESULTS

The dc susceptibility χ [Fig. 2(a)] measured at an applied field of 0.01 T vs temperature is found to obey the Curie-Weiss behavior in the range 10–300 K. An effective magnetic moment of $7.7\mu_B/Gd^{3+}$ obtained from the Curie-Weiss fit is close to the expected value of $7.94\mu_B/Gd^{3+}$ for the free ion $^8S_{7/2}$, and a paramagnetic Curie temperature θ_{CW} of $-9.6(3)$ K indicates antiferromagnetic interactions between the Gd^{3+} spins. It is worth noting that χ starts deviating at a temperature of the order of θ_{CW} as it ought to be for a ''conventional'' system undergoing a transition to long-range order. That θ_{CW} is predominantly due to exchange interactions as opposed to crystal-field effects is confirmed by measurements on the magnetically diluted system $(Gd_{0.02}Y_{0.98})_2Ti_2O_7$, for which θ_{CW} is much reduced and of the order of ~ -0.9 K [Fig. 2(b)]. The absence of any magnetic ordering down to 2 K in the concentrated system, even though θ_{CW} is about five times larger than this temperature, suggests the presence of important magnetic frustration inhibiting the occurrence of magnetic long-range order.

In search of a possible magnetic ordering below 2 K, ac susceptibility χ_{ac} was measured down to 0.3 K. The temperature variation of χ_{ac} for different frequencies (Fig. 3) exhibits two features, a broad peak centered at about 2 K and a sharp down turn below about 1 K, the latter possibly signaling a transition to long-range antiferromagnetic order. $\chi_{ac}(\omega)$ appears to be independent of frequency that would seem to rule
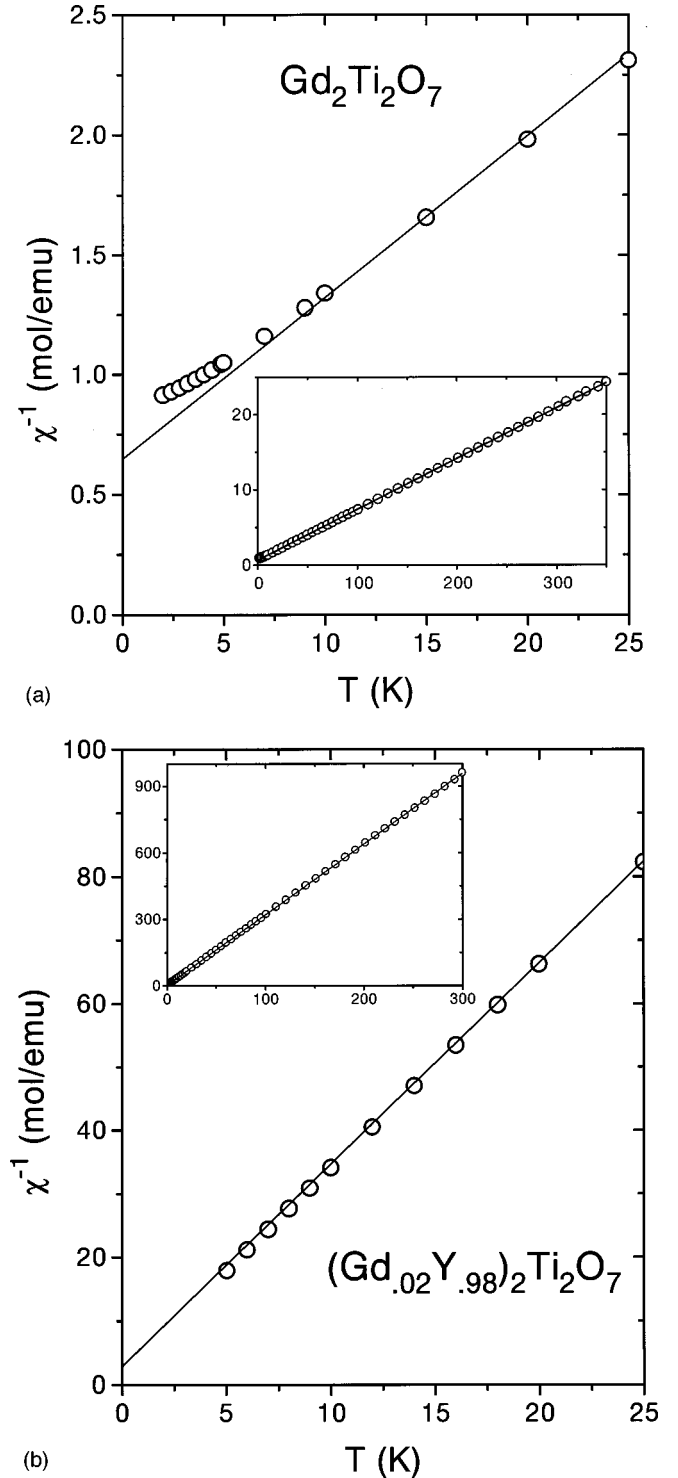

(a)

(b)

FIG. 2. (a) Inverse molar susceptibility $1/\chi$ of $Gd_2Ti_2O_7$ against temperature in the temperature range $T=2-25$ K, and in the temperature range $T=2-300$ K in the inset. (b) Inverse molar susceptibility $1/\chi$ of $(Gd_{0.02}Y_{0.98})_2Ti_2O_7$ against temperature in the temperature range $T=2-25$ K, and in the temperature range $T=2-300$ K in the inset.

out a spin-glass state, as opposed to what has been found in other pyrochlore oxides such as $Y_2Mo_2O_7$,[22–24] $Tb_2Mo_2O_7$,[22,25] and the frustrated $Gd_3Ga_5O_{12}$ garnet.[9,10,12]

The specific heat C_p as a function of temperature is shown in Fig. 4. There is a broad peak centered around 2 K
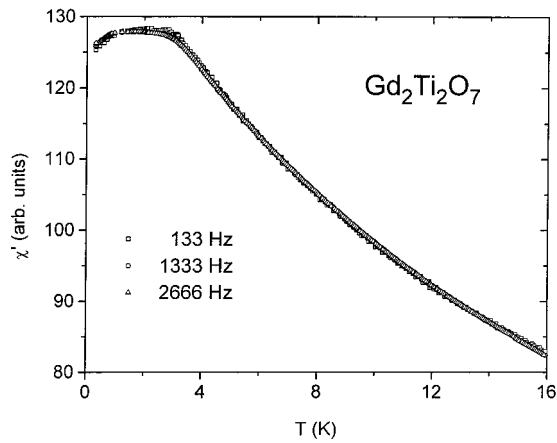
FIG. 3. Real part of the ac susceptibility χ' vs temperature measured at different frequencies.

and a very sharp peak slightly below 1 K indicating the presence of short-range correlations and, in agreement with the ac susceptibility data, the development of long-range magnetic order via a sharp transition at 1 K. The solid line corresponds to the estimated lattice specific heat C_l of $Gd_2Ti_2O_7$, determined by scaling the specific heat for $Y_2Ti_2O_7$, which is insulating, nonmagnetic, and isostructural to $Gd_2Ti_2O_7$. The magnetic specific heat C_m was obtained by subtracting C_l from C_p and its temperature variation is shown in Fig. 5.

The Gd^{3+} ion has an isotropic spin of $S=7/2$ with no orbital magnetic moment contribution and the degeneracy of the eight-level ground state cannot be lifted by the crystal electric field beyond a fraction of a Kelvin. The presence of C_m up to about 30 K clearly indicates that the ground-state degeneracy is lifted by magnetic interactions.

The magnetic entropy S_m was obtained by extrapolating the C_m/T behavior to 0 K and numerically integrating it versus temperature. The total magnetic entropy is 33.8 $J\,mol^{-1}\,K^{-1}$ which is close to the expected $2R\ln(8)=34.6$ $J\,mol^{-1}\,K^{-1}$ for an $S=7/2$ system. The entropy re-
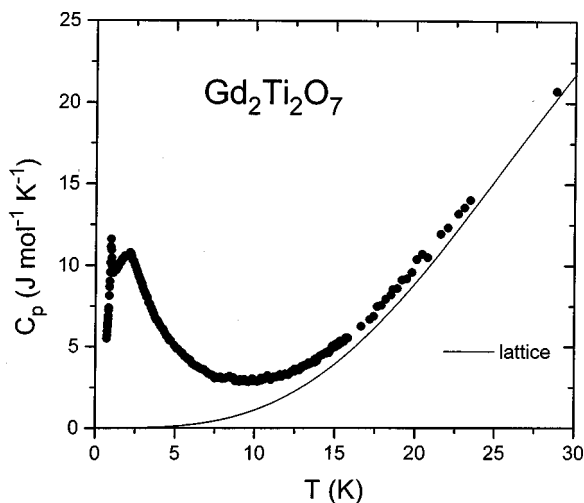

FIG. 4. Specific heat C_p of $Y_2Ti_2O_7$ as function of temperature. The solid line corresponds to the lattice specific heat C_l estimated from the measurements on the nonmagnetic $Y_2Ti_2O_7$.
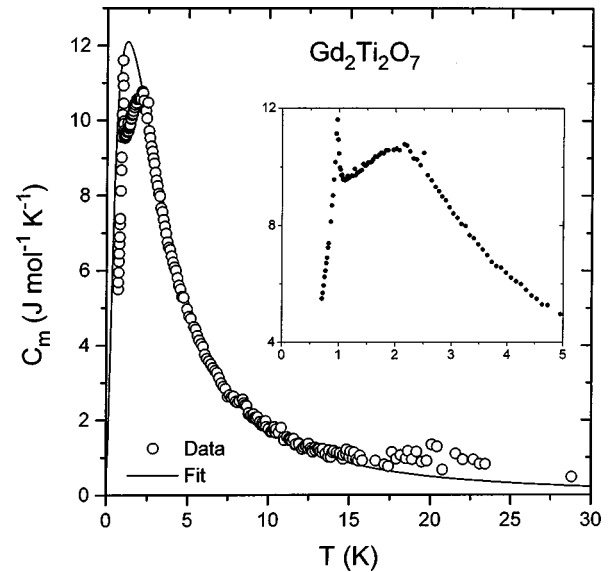

FIG. 5. Magnetic specific heat C_m (obtained by subtracting C_l from C_p) against temperature. The solid line represents the theoretical fit (see text for details). The inset shows a blown-up region of C_m in the low-temperature regime.

covered at the long-range order temperature is about 50% of the total value, which indicates that a sizable fraction of the entropy is due to the short-range correlations present above $T=1$ K.

An attempt was made to fit the C_m data above 1 K. A zeroth-order model consisting of a simple Schottky anomaly based on a splitting scheme of eight equally spaced discrete levels, i.e., assuming a unique value for the internal magnetic field at each Gd^{3+} site, gives a poor fit, as might be expected. A much better fit is obtained by assuming a continuous range of energy-level splittings with a truncated Gaussian distribution. The probability distribution is normalized such that the area under the curve is unity. The resulting fit is shown in Fig. 5. This model is equivalent to assuming a distribution of internal magnetic fields, i.e., an array of random fields as appropriate to a thermal regime dominated by quasistatic short-range magnetic order. A similar approach has been used before to model the specific-heat anomaly due to the Gd sublattice in $Gd_2Mo_2O_7$.[37] In this pyrochlore structure material the Mo^{4+} sublattice undergoes a spin-glass type of order at 60 K while the Gd^{3+} specific-heat contribution is a broad peak centered about 9 K.

In summary, experimental results obtained from ac and dc susceptibility measurements as well as specific-heat measurements give strong compelling evidence for a single sharp transition to a long-range-ordered state at $T_c=0.97$ K preceded by a short-range-ordered regime that extends to approximately $30T_c \sim 3\theta_{CW}$. The heat capacity in this regime can be modeled in terms of a distribution of random exchange fields acting on the $^8S_{7/2}$ ground state of Gd^{3+}.

IV. MEAN-FIELD THEORY

A. Model and method

Our aim in this section is to determine, within mean-field theory, what the expected magnetic properties and type of magnetic-ordered phase(s) for a classical spin model of $Gd_2Ti_2O_7$ are.

We first consider the following classical spin Hamiltonian for $Gd_2Ti_2O_7$:

$$H = \frac{1}{2} \sum_{(i,j)} -J_{ij} \mathbf{S_i} \cdot \mathbf{S_j} + \frac{1}{2} \sum_{(i,j)} \left(\frac{\boldsymbol{\mu}_i \cdot \boldsymbol{\mu}_j}{r_{ij}^3} - 3 \frac{\boldsymbol{\mu}_i \cdot \mathbf{r}_{ij} \mathbf{r}_{ij} \cdot \boldsymbol{\mu}_j}{r_{ij}^5} \right).$$

(4.1)

The first term is the isotropic Heisenberg exchange interaction, and the second term is the dipolar coupling between the Gd magnetic moments. For the open pyrochlore lattice structure, we expect very small second and further nearest-neighbor exchange coupling, $J_{n \geq 2}$, compared to the nearest neighbor J_1 ($J_{n \geq 2} < 0.05 J_1$).[38] Hence, we first consider the case where the sum in the first (exchange) term of Eq. (4.1) above is restricted to the nearest-neighbor exchange J_1 only.[39]

Gd^{3+} has a spin $S = 7/2$, which gives an effective dipole moment of $\mu(Gd^{3+}) = g \mu_B \sqrt{S(S+1)} = 7.94 \mu_B$, with $g = 2$, in good agreement with the Curie constant determined in Sec. III. This gives an estimate for the nearest-neighbor strength of the dipole-dipole interaction $D_{dd} = 63 \mu_B^2 \mu_0 / (4 \pi r_{nn}^3)$, where μ_0 is the magnetic permeability. With a Gd^{3+} at $\mathbf{r} = (0,0,0)$ and a nearest-neighbor at $\mathbf{r}_{nn} = (a/4, a/4, 0)$, where $a = 10.184$ Å is the size of the conventional cubic unit cell, we find $D_{dd} \approx 0.84$ K.

An estimate of the nearest-neighbor exchange J_1 can be found from the measured Curie-Weiss temperature (see below). We have $\theta_{CW} \sim -9.6$ K. This gives for the effective classical nearest-neighbor exchange, $J_1^{cl} = J_1 S(S+1) \sim -4.8$ K using $\theta_{CW} = z J_1 S(S+1)/3$, where $z = 6$ is the number of the nearest neighbor. We henceforth use a classical approximation of Eq. (4.1) above, where we use unit length vectors $\mathbf{S}_i$, and replace $\boldsymbol{\mu}_i$ by $\mathbf{S}_i (D_{dd})^{1/2}$, and express r_{ij} in units of the nearest-neighbor distance. We set $J_1 = -4.8$ K and a strength of 0.84 K for the nearest-neighbor dipole coupling. Below, we take $D_{dd}/J_1 = 0.2$.[40] Hence, unlike in the transition-metal pyrochlores, dipole-dipole interactions is the major perturbation at play beyond the nearest-neighbor Heisenberg exchange coupling in $Gd_2Ti_2O_7$.

We now proceed along the lines of Reimers, Berlinskly, and Shi in their mean-field study of Heisenberg pyrochlore antiferromagnets.[13] We consider the mean-field order parameters, $\mathbf{B}(\mathbf{r}_i)$ at site $\mathbf{r}_i$, in terms of Fourier components. The pyrochlore lattice is a non-Bravais lattice, and we use a rhombohedral basis where there are four atoms per unit cell located at $(0,0,0)$, $(1/4, 1/4, 0)$, $(1/4, 0, 1/4)$, and $(0, 1/4, 1/4)$ in units of the conventional cubic unit cell. We relabel the spins, $\mathbf{S}(\mathbf{r}_i)$, in terms of unit cell coordinates, and a sublattice index within the unit cell, and take advantage of the translational symmetry of the lattice, and expand the order parameters $\mathbf{B}(\mathbf{r}_i)$ in terms of Fourier components. In this case $\mathbf{B}^a(\mathbf{r}_i)$ on the ath sublattice site of the unit cell located at $\mathbf{r}_i$ can be written as

$$\mathbf{B}^a(\mathbf{r}_i) = \sum_{\mathbf{q}} \mathbf{B}^a(\mathbf{q}) \exp(i \mathbf{q} \cdot \mathbf{r}_i).$$

(4.2)

The spin-spin interaction matrix $\mathcal{J}_{\alpha\beta}(|\mathbf{r}_{ij}|)$, including both exchange and dipolar interactions, reads

$$\mathcal{J}_{\alpha\beta}^{ab}(|\mathbf{r}_{ij}|) = J_1 \delta_{\alpha\beta} \delta_{r_{ij}, r_{nn}} + D_{dd} \left\{ \frac{\delta_{\alpha\beta}}{(r_{ij}^{ab})^3} - 3 \frac{r_{ij,\alpha}^{ab} r_{ij,\beta}^{ab}}{(r_{ij}^{ab})^5} \right\},$$

(4.3)

where $\delta_{\alpha\beta}$ is the Kronecker delta, and α and β refer to the x, y, z Cartesian components of $\mathbf{S}_i$ and $\mathbf{r}_{ij}^{ab}$. $r_{ij,\alpha}^{ab}$ denotes the α components of the interspin vector $\mathbf{r}_{ij}$ that connects spin $\mathbf{S}_i^a$ to spin $\mathbf{S}_j^b$. We write $\mathcal{J}_{\alpha\beta}$ in terms of its Fourier components as

$$\mathcal{J}_{\alpha\beta}^{ab}(|\mathbf{r}_{ij}|) = \frac{1}{n} \sum_{\mathbf{q}} \mathcal{J}_{\alpha\beta}^{ab}(\mathbf{q}) \exp(-i \mathbf{q} \cdot \mathbf{r}_{ij}),$$

(4.4)

where N is the number of unit cells with four spins per unit cell.

The quadratic part of the mean-field free-energy $F^{(2)}(T)$ then becomes[13]

$$F^{(2)}/N = \frac{1}{2} \sum_{\mathbf{q},(ab),(\alpha\beta)} B_\alpha^a(\mathbf{q}) \{ 3T \delta_{ab} \delta_{\alpha\beta} - \mathcal{J}_{\alpha\beta}^{ab}(\mathbf{q}) \}$$
$$\times B_\beta^b(-\mathbf{q}).$$

(4.5)

Diagonalizing $F^{(2)}(T)$ requires transforming to normal modes of the system

$$B_\alpha^a(\mathbf{q}) = \sum_i \sum_\beta U_{\alpha\beta}^{a,i} \Phi_\beta^i(\mathbf{q}),$$

(4.6)

where $\Phi_\beta^i(\mathbf{q})$ are the eigenmodes, and $U(\mathbf{q})$ is the unitary matrix that diagonalizes $\mathcal{J}(\mathbf{q})$ in the spin-sublattice space, with eigenvalues $\lambda(\mathbf{q})$,

$$\sum_b \sum_\beta \mathcal{J}_{\alpha\beta}^{ab}(\mathbf{q}) U_{\beta\gamma}^{bi}(\mathbf{q}) = \lambda_\gamma^i(\mathbf{q}) U_{\alpha\gamma}^{ai}(\mathbf{q}).$$

(4.7)

Henceforth we will use the convention that indices (ab) label sublattices, that indices (ijk) label the normal modes, and that $(\alpha\beta\gamma)$ labels spin components. We express $F^{(2)}(T)$ in terms of normal modes

$$F^{(2)}/N = \frac{1}{2} \sum_{\mathbf{q}} \sum_i \sum_\gamma \Phi_\gamma^i(\mathbf{q}) \Phi_\gamma^i(-\mathbf{q}) \{ 3T - \lambda_\gamma^i(\mathbf{q}) \}.$$

(4.8)

The first-ordered state of the system occurs at the temperature

$$T_c = \frac{1}{3} \max_{\mathbf{q},i,\alpha} \{ \lambda_\alpha^i(\mathbf{q}) \},$$

(4.9)

where $\max_{\mathbf{q},i,\alpha} \{ \lambda_\alpha^i(\mathbf{q}) \}$ indicates a global maximum of the spectrum of $\lambda_\alpha^i(\mathbf{q})$ for all $\mathbf{q}$.

Let us briefly explain how we proceed using the above set of equations to determine the "soft mode(s)" of the system at T_c. First, the Fourier transform of $\mathcal{J}_{\alpha\beta}^{ab}(|\mathbf{r}_{ij}|)$ is calculated using Eq. (4.3).[41] For the rhombohedral basis used above, the space is of dimension $\mathcal{D}_\mathbf{S} \otimes \mathcal{D}_{sl}$, where the spin-component subspace $\mathcal{D}_\mathbf{S}$ is of dimension 3×3 and the sublattice subspace $\mathcal{D}_{sl}$ is of dimension 4×4. The eigenvalues $\{ \lambda_\alpha^i(\mathbf{q}) \}$ and eigenvectors $\Phi_\alpha^i(\mathbf{q})$ are determined by reshaping $\mathcal{J}_{\alpha\beta}^{ab}(\mathbf{q})$ into a 12×12 array. The pyrochlore lattice has a

symmetry of inversion with respect to a lattice point and this implies that $\mathcal{J}_{\alpha\beta}^{ab}(\mathbf{q})$ is real and symmetric. The eigenvalues and eigenvectors are found using a standard numerical package for eigenproblems of real symmetric matrices.

B. Results

For $D_{dd}=0$, we recover the results of Ref. 13. Before we present the results with the dipolar interactions, we review the mean-field results found for the isotropic pyrochlore class Heisenberg antiferromagnet depending on the values of the second, J_2, and third, J_3, nearest-neighbor exchange couplings.[13] For $J_2=J_3=0$ there are two dispersionless unstable or critical modes throughout the Brillouin zone. There are therefore no selected wave vectors for long-range order. Numerical work has shown that no long-range order occurs at nonzero temperature in the nearest-neighbor classical Heisenberg pyrochlore antiferromagnet.[14,15] For $J_3=0$, ferromagnetic $J_2>0$ gives rise to an ordering at an incommensurate wave vector, while for antiferromagnetic $J_2<0$, the system orders at $\mathbf{q}^*=0$. For $J_2=0$ and ferromagnetic $J_3>0$, the system also orders at $\mathbf{q}^*=0$, while there are dispersionless (degeneracy lines) along certain symmetry directions for $J_2=0$ and antiferromagnetic $J_3<0$. In the overall parameter space $\{J_2/J_1,J_3/J_1\}$, long-range order is always expected to occur at nonzero temperature within mean-field theory, except for $J_2\equiv0$ and antiferromagnetic $J_3\leq0$ (Fig. 6 in Ref. 13).

We now consider the case where $D_{dd}/J_1=0.2$, and first set $J_2=J_3=0$. Naively, one might have thought that (i) the long range and (ii) anisotropic nature of the dipolar interactions would lift *all* macroscopic ground-state degeneracies that occur in the isotropic nearest-neighbor ($J_1<0$) Heisenberg antiferromagnet and give rise to a uniquely selected wave vector $\mathbf{q}^*$, at which long-range order would occur.[13] This is not the case. We find that the largest eigenvalue $\lambda_\alpha^i(\mathbf{q})$ that controls the mean field T_c [Eq. (4.9)] is dispersionless along the star of the [111] direction in the cubic basis (Fig. 6). The figure shows $\lambda_{max}(\mathbf{q})$ as a function of $\mathbf{q}_1$ in the [110] and $\mathbf{q}_2$ in the [001], where $\lambda_{max}(\mathbf{q})$ is the largest eigenvalue of $\lambda_\alpha^i(\mathbf{q})$ at a given $\mathbf{q}$. Hence, no long-range order is to be expected in this system within the mean-field approximation.[41] In this context, it is interesting to note that the combined *long-range* dipolar *and* Ruderman-Kittel-Kasuya-Yosida interactions in the problem of nuclear magnetism in Cu and Ag do not lead either to a full selection of a unique classical long-range-ordered state below the mean field T_c.[42] Such "degeneration lines" as found in the present system also occur in other frustrated systems such as the nearest-neighbor Heisenberg fcc antiferromagnet where there are degeneration lines along the $\pi/a(1,q,0)$ direction.[16–18] Degeneration (spiral) lines also occur in the more complicated case of the rhombohedral antiferromagnet.[43] By analogy with the work on the frustrated fcc (Refs. 16–18, and 42) and rhombohedral[43] antiferromagnets, we expect that for degeneration lines (as opposed to degeneration *zone* as in the case of the nearest-neighbor pyrochlore antiferromagnet[13,14]), thermal and/or quantum fluctuations will restore long-range order at finite temperature via a process of order by disorder. Work in that direction is in progress and will be reported elsewhere.[39]
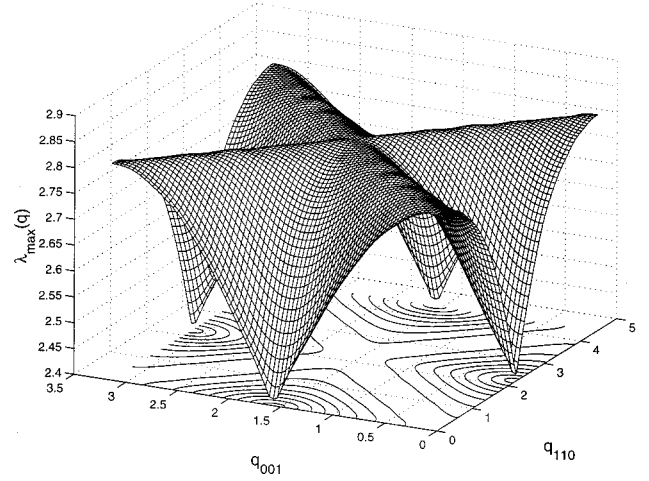

FIG. 6. Largest eigenvalue $\lambda_{max}(\mathbf{q})$ as a function of wave vector $\mathbf{q}$ for $D_{dd}/J_1=0.2$ and $J_2=J_3=0$. A degeneration line occurs for $\mathbf{q}$ in the star of the [111] direction. The small "ripples" seen on the degeneration lines along (111) and (11$\bar{1}$) directions are due to the finite number (500) of nearest neighbors considered in the dipolar interactions. When considering more than ten nearest neighbors, the maximum of $\lambda(\mathbf{q})$ always occurs on the star of [111] with the amplitude of the modulations due to the dipolar cutoff continuously decreasing as the number of nearest neighbors is increased to infinity.

We find that for either nonzero ferromagnetic or antiferromagnetic, $|J_2|\ll D_{dd}$ and/or $|J_3|\ll D_{dd}$, that the line degeneracy along the [111] direction is lifted and that a specific value q^* along that direction is picked up, giving rise to an absolute maximum of $\lambda_\alpha^i(\mathbf{q})$. For sufficiently large $|J_2|$ and/or $|J_3|$ compared to D_{dd}, a different selected wave-vector direction is chosen, as found by Reimers *et al.*,[13] except that here there is no degeneration line occurring for $J_2=0$ and $J_3<0$, as found in Ref. 13 when $D_{dd}\neq0$, $D_{dd}\ll|J_2|$, and $D_{dd}\ll|J_3|$. In other words, all nonglobal degeneracies are lifted in the case where $D_{dd}\neq0$, $J_2\neq0$, and $J_3\neq0$.

In summary, we would expect that long-range order should occur in $Gd_2Ti_2O_7$, either via an order-by-disorder mechanism, or via energetic selection of an ordering wave vector via superexchange couplings beyond J_1 and dipolar interactions D_{dd}.

V. DISCUSSION

It is useful to compare $Gd_2Ti_2O_7$ with related systems such as the remaining $R_2Ti_2O_7$ materials, $Gd_3Ga_5O_{12}$ (GGG), Gd_2O_3, cubic-Gd_2O_3 (C-Gd_2O_3), and also $GdAlO_3$ for reasons that should soon become clear.

C-Gd_2O_3 crystallizes in the so-called bixbyite structure $Ia3$ with two distinct crystallographic sites. However, the sublattice of the two sites taken together is an excellent approximation to an fcc lattice. Its properties are as follows: Curie-Weiss behavior is observed with $\theta_{CW}=-17$ K, but magnetic order of undetermined range is not found down to 1.6 K.[44] In fact, the description of the neutron-diffraction data for C-Gd_2O_3 bears a striking resemblance to that for GGG.[11] The heat capacity from 1.4 to 18 K shows only a broad "Schottky"-type anomaly peaked near 2 K with mag-

netic contributions extending to about 20 K.[44] Neutron-diffraction data in the form of diffuse scattering confirm that the short-range magnetic correlations do extend to at least 20 K.[44] It is clear that C-Gd_2O_3 should be reconsidered as a geometrically frustrated antiferromagnet material although the original interpretation of its properties was not presented in those terms. In particular, it is important to determine whether C-Gd_2O_3 does indeed undergo true long-range order, as seems to be the case for $Gd_2Ti_2O_7$, and if the susceptibility is frequency dependent.

GGG has been recognized as a geometrically frustrated antiferromagnet since 1979.[8] Its properties are an amalgam of those of $Gd_2Ti_2O_7$ and C-Gd_2O_3 scaled to lower energies. For example, $\theta_{CW} = -2.3$ K and the maximum in the heat capacity occurs at 0.8 K. True long-range order is not established down to 43 mK but incommensurate short-range order on a ~ 100-Å length scale is found at the lowest temperature studied.[11] The extended short-range order starts developing rapidly at ~ 140 mK, which is close to the temperature at which the nonlinear coefficient $\chi_3(T)$ peaks as found in Ref. 10. Coexistence of spin-glass and long-range order in the form of a frequency-dependent susceptibility is found, which contrasts sharply with the lack thereof in $Gd_2Ti_2O_7$. At this point it is useful to point out that $Gd_2Ti_2O_7$, GGG, and C-Gd_2O_3 represent anomalies in the context of magnetic Gd^{3+} oxides. For example, monoclinic Gd_2O_3 in which the Gd sublattice is not fcc, unlike C-Gd_2O_3, is a normal antiferromagnet with $T_c = 3.8$ K and greater than 90% entropy removal below T_c.[45] In $GdAlO_3$, the Gd ions are on a simple cubic lattice and $\theta_{CW} = -4.8$ K, $T_c = 3.8$ K, and nearly 100% of the entropy is removed below T_c.[45]

At present, the strong contrast in behavior between $Gd_2Ti_2O_7$ and GGG remains unexplained. On the subject of why $Gd_2Ti_2O_7$ orders and GGG does not, one can only speculate. For example, for the very specific topology of the garnet lattice, there may remain degenerate or quasidegenerate dispersion lines or surfaces of zero mode in q space that survive even upon the inclusion of perturbations such as dipolar and or higher than first-neighbor exchange interactions. Thus the selection of an ordering wave vector q^* for GGG may be much less robust than for the much different topology presented by $Gd_2Ti_2O_7$ for perturbations $\{H'\}$ of similar order of magnitude.[39]

Returning to the $R_2Ti_2O_7$ series, as mentioned, $Gd_2Ti_2O_7$ offers the opportunity to study a system in which the crystal-field and anisotropy perturbations are minimized. As this is certainly not the case for $R = $ Tb, Ho and Tm, some comment on the symmetry of the local environment at the R site is in order. The $16d$ rare-earth site is coordinated by two sets of oxygen atoms, six O1($48f$) and two O2($8b$), giving eight-fold coordination overall. It is important to note that the R site symmetry is strongly distorted from cubic, which would imply eight equal R-O distances (for $R = $ Gd, the sum of the ionic radii gives 2.42 Å) and O-R-O angles of 70.5°, 109.5°, and 180°. In $R_2Ti_2O_7$, the six O1 atoms form a puckered ring about the R (Gd-O distance of 2.55 Å) and the two O2 atoms a linear O2-R-O2 unit oriented normal to the mean plane of the puckered ring with extremely short R-O2 distances (Gd-O distance is 2.21 Å). This Gd-O distance is among the shortest, if not the shortest, such distance known in Gd-oxide chemistry and implies a very strong interaction.

TABLE I. Presence or absence of long-range order in $R_2Ti_2O_7$ pyrochlores.

Rare earth	n in $4f^n$	Long-range order (T_c)	Ref.
Gd	7	YES, (0.97 K)	This work
Tb	8	NO	Refs. 34 and 35
Dy	9	NO	Refs. 47, 48, and 49
Ho	10	NO	Refs. 31, 48, and 49
Er	11	YES, (1.25 K)	Ref. 47
Tm	12	NO	Refs. 29 and 30
Yb	13	YES, (0.21 K)	Refs. 47, 48, and 49

This observation suggests that a crystal field of axial symmetry might be an even better approximation than cubic. The O2-Gd-O2 angle is, of course, 180° while the O1-Gd-O1 angles are 62.7°, 117°, and 180°, and the O1-Gd-O2 angles are 81° and 100°. Thus, it is best, when thinking about the R site crystal field, to consider the true symmetry, $-3m(D_3d)$, rather than relying on cubic or axial approximations.

The known situation with respect to the presence or absence of long-range order in the $R_2Ti_2O_7$ pyrochlores is summarized in Table I. One obvious correlation is that those $R_2Ti_2O_7$ pyrochlores that contain a Kramers (odd electron) ion nearly always show long-range order (Dy being the exception) while those with a non-Kramers (even electron) ion do not. A "zeroth-order" interpretation of the trends in Table I is then that the action of the relatively low-symmetry crystal field induces a true singlet ground state in the non-Kramers ions and this is the explanation of the absence of long-range order (LRO). There is good evidence that such is the case for $R = $ Tm from a combination of susceptibility,[29,30] inelastic neutron scattering,[30] and crystal-field calculations (using the correct $-3m$ symmetry).[46] Experimentally,[30] the singlet state is well separated by 120 K from the nearest excited state, which is in remarkable agreement with the aforementioned crystal-field calculations that predict 118 K.[46]

The other two non-Kramers ions are not so simple. For $Ho_2Ti_2O_7$ the ground state is thought to be an Ising doublet,[32] in agreement with crystal-field calculations,[46] and the nearest-neighbor exchange is weakly ferromagnetic. Here it has been argued that the strong Ising-like single-ion anisotropy along the [111] frustrates the development of long-range ferromagnetic order.[31,32] However, recent studies suggest a more complex picture where dipolar interactions competing with *antiferromagnetic* exchange are responsible for the behavior observed in $Ho_2Ti_2O_7$.[49] This material also exhibits spin dynamics and spin freezing reminiscent of the disorder-free, intrinsic glassy behavior exhibited by the "ice model"[31,32] with an exponential decrease of the spin-lattice relaxation rate suggestive of Orbach processes.[33] In contrast, $Gd_2Ti_2O_7$ exhibits no apparent dynamics or spin glassiness at any temperature even above T_c.

A detailed study of $Tb_2Ti_2O_7$ will be described in a subsequent publication.[35] The salient facts are that the Tb^{3+} ground state also appears to be a doublet but not so well isolated from several other levels within 15–100 K. The exchange interactions are relatively strongly antiferromagnetic, comparable to $Gd_2Ti_2O_7$, and short-range magnetic correla-

tions persist up to at least 30 K, also similar to what is found in $Gd_2Ti_2O_7$. $Tb_2Ti_2O_7$ does not order down to 70 mK.[34] The lack of LRO in this system is difficult to understand.[35] Indeed, as argued in Refs. 20 and 50, a nearest-neighbor Heisenberg antiferromagnet with a [111] easy axis is a trivial problem with an effectively nonfrustrated and unique (twofold Ising-like globally degenerate) classical ground state, and should therefore show a phase transition at non-zero temperature in the limit of sufficiently strong crystal-field level splitting compared to the superexchange J.

From the above discussion we can conclude that each $R_2Ti_2O_7$ material presents its own special set of circumstances where details of the finely tuned relative strength of crystal-field parameters, exchange, and dipolar couplings play a crucial role, and a blanket explanation for the apparent systematics of Table I will not be found. It is worth noting an interesting paradox. $Gd_2Ti_2O_7$ represents the case for which some of the perturbations that might be thought to aid in the selection of a unique ground state, i.e., crystal fields and anisotropy, are largely absent, yet it orders. On the other hand, $Tb_2Ti_2O_7$ and $Ho_2Ti_2O_7$, in which crystal fields and anisotropy are clearly important, do not order and it is likely that these perturbations, in fact, inhibit the occurrence of long-range order by competing with important interactions *other*[49] than nearest-neighbor Heisenberg antiferromagnetic exchange.[20,32,50] Some other interesting recent results have been found in the $Yb_2Ti_2O_7$ and $Dy_2Ti_2O_7$ pyrochlores.[48]

It is also useful to compare $Gd_2Ti_2O_7$ with other Heisenberg pyrochlores such as $Y_2Mo_2O_7$ (Refs. 22–24) and Heisenberg spinels such as $ZnFe_2O_4$.[51] $Y_2Mo_2O_7$ is a well-known geometrically frustrated antiferromagnet spin-glass material with $\theta_{CW}/T_f \gtrsim 10$, T_f being the spin freezing temperature of 21 K.[23] Here too, only a speculation can be offered for the differences as follows: Because of the high level of degeneracy across the zone, the nearest-neighbor Heisenberg pyrochlore antiferromagnet is expected to be fragile against a small random disorder level x, and will have a propensity to develop a *disorder-driven* spin-glass ground state the smaller the perturbations $\{H'\}$ beyond the nearest-neighbor exchange interaction.[7,20] We expect that the critical disorder level for the Néel to spin-glass transition x_c will go to zero as $\{H'\}$ goes to zero.[7] For example, in $Y_2Mo_2O_7$, there is preliminary evidence that the second-neighbor exchange parameter J_2 is only a few percent of J_1.[52] In $Gd_2Ti_2O_7$, on the other hand, the leading corrections $\{H'\}$ are dipolar interactions D_{dd} and of order 20% of J_1. In other words $\{H'\}/J_1$ is not small in $Gd_2Ti_2O_7$ and the anisotropy of the dipolar interactions will possibly introduce sizable stabilizing anisotropy gaps to the spin-wave excitations out of the selected long-range-ordered ground state. Both the relative size of D_{dd}/J_1 and the ''spin-holding'' effect of the anisotropy of dipolar interactions will result in a much increased x_c compared to more isotropic Heisenberg systems with small $\{H'\}$.[7] In summary, in this picture weak disorder drives the spin-glass transition in $Y_2Mo_2O_7$, while the strong and anisotropic dipolar interaction ''helps'' stabilize long-range order in $Gd_2Ti_2O_7$. In this context the existence of a very weakly dispersive line along [111] restored by order by disorder, or perturbative J_2 and J_3, would suggest that, as in the fcc antiferromagnet,[16] weak random disorder would rapidly drive $Gd_2Ti_2O_7$ into a spin-glass state.

Finally, it is interesting to compare the behavior of $Gd_2Ti_2O_7$ with the frustrated $ZnFe_2O_4$ antiferromagnet spinel, where Fe^{3+} is a $^6S_{5/2}$ closed-shell ion for which single-ion anisotropy should be negligible as is the case for the $^8S_{7/2}$ Gd^{3+} ion in $Gd_2Ti_2O_7$. In the insulating normal Heisenberg spinel $ZnFe_2O_4$, where the Fe^{3+} magnetic moments occupy a lattice of corner-sharing tetrahedra, muon spin relaxation and neutron studies have revealed that long-range antiferromagnetic order develops below $T_N = 10.5$ K. However, already at temperatures of about $T \approx 10T_N$ a short-range antiferromagnetic order (SRO) develops that extends through $\approx 70\%$ of the sample volume just above T_N. Below T_N antiferromagnetic SRO and LRO coexist. At 4.2 K, still $\approx 20\%$ of the sample are short-range ordered. The regions exhibiting SRO are very small, ≈ 30 Å. The physical origin of the SRO as well as partial glassy behavior in $ZnFe_2O_4$ remains an enigma. Hence, while it appears that $Gd_2Ti_2O_7$ displays conventional antiferromagnetic long-range order and $Y_2Mo_2O_7$ shows full-blown spin-glass behavior, $ZnFe_2O_4$ exhibits a combination of both short- and long-range antiferromagnetic order, as well as spin-glass behavior. The origin of the difference between the Gd- and Fe-based pyrochlore lattice antiferromagnets in terms of their coexistence of long-range order and spin-glass behavior is not known. Possibly different range of interactions, the presence of strong dipolar anisotropy in $Gd_2Ti_2O_7$ compared to a much more overall isotropic spin-spin interaction in $ZnFe_2O_4$ may play some role. In light of this, it would be interesting to study in further detail the magnetic properties of $Gd_2Ti_2O_7$ using muon spin relaxation and neutron-scattering methods.

VI. CONCLUSION

Evidence has been presented from ac and dc susceptibility and specific-heat measurements, that the frustrated $Gd_2Ti_2O_7$ insulating pyrochlore exhibits a transition to a long-range-ordered state at 0.97 K as opposed to a spin-glass or spin-liquid state as often observed in other pyrochlore materials. From specific-heat measurements, short-range magnetic correlations have been found to extend to $T > 30T_c$ and the entropy removal below T_c is only about 50%. From a mean-field theoretical study it is concluded that no long-range order should exist for the pyrochlore lattice for nearest-neighbor antiferromagnetic interactions J_1 only, even upon inclusion of long-range anisotropic dipolar couplings D_{dd}. Long-range order at various commensurate or incommensurate wave vectors is predicted to occur only upon including a finite second, J_2, and/or third, J_3, nearest-neighbor exchange interactions beyond J_1 and D_{dd}. Long-range order could also be driven by thermal and/or quantum fluctuations via an order-by-disorder mechanism. The exact wave vector depends on the relative signs and magnitudes of J_2, J_3, and D_{dd}. It would be of interest to investigate further the nature of the ordered state in zero and applied fields in $Gd_2Ti_2O_7$ by neutron scattering and muon spin-relaxation methods. Finally, we argued above that the related fcc antiferromagnet material, cubic-Gd_2O_3, should be reconsidered as a geometrically frustrated antiferromagnet and is worthy of further study.

*Present address: Department of Physics, The Ohio State University, Columbus, OH 43210-1106.

†Present address: Serin Physics Laboratory, Rutgers University, Piscataway, NJ 08555-0849.

‡Permanent address: Department of Physics, University of Waterloo, Waterloo, Ontario, Canada N2L 3G1.

§Present address: Spallation Neutron Source, Oak Ridge National Laboratory, 104 Union Valley Rd., SNS Bldg., Oak Ridge, TN 37831-8218.

[1] P. Schiffer and A. P. Ramirez, Comments Condens. Matter Phys. **18**, 21 (1996); *Magnetic Systems with Competing Interactions*, edited by H. T. Diep (World Scientific, Singapore, 1994); M. J. P. Gingras (unpublished).

[2] P. Chandra and P. Coleman, *New Outlooks and Old Dreams in Quantum Antiferromagnets*, Les Houches Summer School Lectures, edited by B. Douçot and J. Zinn-Justin (North-Holland, Amsterdam, 1991).

[3] P. Lecheminant, B. Bernu, C. Lhuillier, L. Pierre, and P. Sindzingre, Phys. Rev. B **56**, 2521 (1997); Ch. Waldtmann, H.-U. Everts, B. Bernu, P. Sindzingre, P. Lecheminant, and L. Pierre, Eur. Phys. J. B **2**, 501 (1998), and references therein; F. Mila, Phys. Rev. Lett. **81**, 2356 (1998).

[4] B. Canals and C. Lacroix, Phys. Rev. Lett. **80**, 2933 (1998), and references therein.

[5] G. Toulouse, Commun. Phys. **2**, 115 (1977).

[6] J. M. D. Coey, Can. J. Phys. **65**, 1210 (1987).

[7] J. Villain, Z. Phys. B **33**, 31 (1978).

[8] W. I. Kinney and W. P. Wolf, J. Appl. Phys. **50**, 2115 (1979); S. Hov, H. Bratsberg, and A. T. Skjeltorp, J. Magn. Magn. Mater. **15-18**, 455 (1980).

[9] P. Schiffer, A. P. Ramirez, D. A. Huse, and A. J. Valentino, Phys. Rev. Lett. **73**, 2500 (1994).

[10] P. Schiffer, A. P. Ramirez, D. A. Huse, P. L. Gammel, U. Yaron, D. J. Bishop, and A. J. Valentino, Phys. Rev. Lett. **74**, 2379 (1995).

[11] O. A. Petrenko, C. Ritter, M. Yethiraj, and D. McK Paul, Phys. Rev. Lett. **80**, 4570 (1998); O. A. Petrenko, D. McK Paul, C. Ritter, T. Zeiske, and M. Yethiraj, *Proceedings of the 4th International Workshop on Quasi-Inelastic Neutron Scattering (QENS98), Nykoping, Sweden* [Physica B **41**, 266 (1999)].

[12] Y. K. Tsui, C. A. Burns, J. Snyder, and P. Schiffer (unpublished).

[13] J. N. Reimers, A. J. Berlinsky, and A.-C. Shi, Phys. Rev. B **43**, 865 (1991).

[14] R. Moessner and J. T. Chalker, Phys. Rev. Lett. **80**, 2929 (1998); Phys. Rev. B **58**, 12 049 (1998).

[15] J. N. Reimers, Phys. Rev. B **45**, 7287 (1992).

[16] W. Minor and T. M. Giebultowicz, J. Phys. (Paris), Colloq. **49**, C8-1551 (1988); H. T. Diep and H. Kawamura, Phys. Rev. B **40**, 7019 (1989); C. Wengel, C. L. Henley, and A. Zippelius, *ibid.* **53**, 6543 (1995), and references therein.

[17] B. E. Larson and C. L. Henley (unpublished).

[18] M. T. Heinila and A. S. Oja, Phys. Rev. B **48**, 16 514 (1993), and references therein.

[19] J. N. Reimers, J. E. Greedan, and M. Björgvinsson, Phys. Rev. B **45**, 7295 (1992); J. A. Mailhot and M. L. Plumer, *ibid.* **48**, 9881 (1993).

[20] S. T. Bramwell, M. J. P. Gingras, and J. N. Reimers, J. Appl. Phys. **75**, 5523 (1994).

[21] S. Sachdev, Phys. Rev. B **45**, 12 377 (1992).

[22] S. R. Dunsiger, R. F. Kiefl, K. H. Chow, B. D. Gaulin, M. J. P. Gingras, J. E. Greedan, A. Keren, K. Kojima, G. M. Luke, W. A. MacFarlane, N. P. Raju, J. E. Sonier, Y. J. Uemura, and W. D. Wu, Phys. Rev. B **54**, 9019 (1996).

[23] M. J. P. Gingras, C. V. Stager, N. P. Raju, B. D. Gaulin, and J. E. Greedan, Phys. Rev. Lett. **78**, 947 (1997).

[24] J. S. Gardner, B. D. Gaulin, S.-H. Lee, C. Broholm, N. P. Raju, and J. E. Greedan (unpublished).

[25] B. D. Gaulin, J. N. Reimers, T. E. Mason, J. E. Greedan, and Z. Tun, Phys. Rev. Lett. **69**, 3244 (1992).

[26] K. Binder and A. P. Young, Rev. Mod. Phys. **58**, 801 (1986); K. H. Fischer and J. A. Hertz, *Spin Glasses* (Cambridge University Press, Cambridge, 1991).

[27] J. E. Greedan, M. Sato, Yan Xu, and F. S. Razavi, Solid State Commun. **59**, 895 (1986); J. N. Reimers and J. E. Greedan, J. Solid State Chem. **72**, 390 (1988); J. E. Greedan, N. P. Raju, A. Maigna, Ch. Simon, J. S. Pedersen, A. M. Niraimathi, E. Gmelin, and M. A. Subramanian, Phys. Rev. B **54**, 7189 (1996).

[28] C. Heremans, B. J. Wuensch, J. K. Stalick, and E. Prince, J. Solid State Chem. **117**, 108 (1995).

[29] J. E. Greedan, in *Oxydes with Trirutile and Pyrochlore Structures*, edited by H. P. J. Wijn, Landolt-Bornstein, New Series, Group III, Vol. 27, Part g (Springer-Verlag, Berlin, 1992), p. 105.

[30] M. P. Zinkin, M. J. Harris, Z. Tun, R. A. Cowley, and B. M. Wanklyn, J. Phys.: Condens. Matter **8**, 193 (1996).

[31] M. J. Harris, S. T. Bramwell, D. F. McMorrow, T. Zeiske, and K. W. Godfrey, Phys. Rev. Lett. **79**, 2554 (1997); S. T. Bramwell and M. J. Harris, J. Phys.: Condens. Matter **10**, L215 (1998).

[32] M. J. Harris, S. T. Bramwell, P. C. W. Holdsworth, and J. D. M. Champion, Phys. Rev. Lett. **81**, 4496 (1998).

[33] G. Ernst, A. P. Ramirez, A. Hayashi, and R. J. Cava (unpublished).

[34] J. S. Gardner, S. R. Dunsiger, B. D. Gaulin, M. J. P. Gingras, J. E. Greedan, R. F. Kiefl, M. D. Lumsden, W. A. MacFarlane, N. P. Raju, J. E. Sonier, I. Swainson, and Z. Tun, Phys. Rev. Lett. **82**, 1012 (1999).

[35] N. P. Raju, J. S. Gardner, M. Faucher, B. C. den Hertog, B. D. Gaulin, R. J. Chang, M. J. P. Gingras, and J. E. Greedan (unpublished).

[36] J. D. Cashion, A. H. Cooke, M. J. M. Leask, T. L. Thorp, and M. R. Wells, J. Mater. Sci. **3**, 402 (1968).

[37] N. P. Raju, E. Gmelin, and R. K. Kremer, Phys. Rev. B **46**, 5405 (1992). In this work, it is shown that in $Gd_2Mo_2O_7$, it is the *static* randomly frozen Mo magnetic moments that provide a distribution of internal Zeeman splitting of the $^8S_{7/2}$ manifold of Gd^{3+}.

[38] J. E. Greedan, N. P. Raju, A. S. Wills, C. Morin, S. M. Shaw, and

J. N. Reimers, Chem. Mater. **10**, 3058 (1998).

[39] B.C. den Hertog, M. J. P. Gingras, and M. Dion (unpublished).

[40] To obtain a more reliable estimate of D_{dd}/J_1, one should determine the Curie-Weiss contribution from dipole-dipole interactions to the high-temperature limit of χ, and hence θ_{CW}, in order to extract a more precise estimate of J_1. The results of such calculations will be produced elsewhere (Ref. 35). Note that the specific value chosen for D_{dd}/J_1 with $J_2=J_3=0$ does not affect the results of a line of degeneracy along the star of [111] (Ref. 39).

[41] We have found that the results for the selected wave vector(s) at the mean-field level depend sensitively on the range of dipolar interactions considered. Here, we have included the first 500 nearest neighbors in the dipolar sum.

[42] P. Hakonen, O. V. Lounasmaa, and A. Oja, J. Magn. Magn. Mater. **100**, 394 (1991).

[43] E. Rastelli and A. Tassi, J. Phys. C **19**, L423 (1986); **21**, L35 (1988).

[44] H. R. Child, R. M. Moon, L. J. Raubenheimer, and W. C. Koehler, J. Appl. Phys. **38**, 1381 (1967); R. M. Moon and W. C. Koehler, Phys. Rev. B **11**, 1609 (1975).

[45] J. D. Cashion, A. H. Cooke, T. L. Thorpe, and M. R. Wells, Proc. R. Soc. London, Ser. A **318**, 473 (1970).

[46] M. Faucher (private communication).

[47] H. W. J. Blöte, R. F. Wielinga, and W. J. Huiskamp, Physica (Amsterdam) **43**, 549 (1969).

[48] A. P. Ramirez, A. Hayashi, R. J. Cava, R. Siddharthan, and B. S. Shastry (unpublished).

[49] R. Siddharthan, B. S. Shastry, A. P. Ramirez, A. Hayashi, R. J. Cava, and S. Rosenkranz, cond-mat/9902010 (unpublished).

[50] R. Moessner, Phys. Rev. B **57**, R5587 (1998).

[51] W. Schiessl, W. Potzel, H. Karzel, M. Steiner, G. M. Kalvius, A. Martin, M. K. Krause, I. Halevy, J. Gal, W. Schdfer, G. Will, M. Hillberg, and R. Wäppling, Phys. Rev. B **53**, 9143 (1996).

[52] N. P. Raju, M. J. P. Gingras, I. A. Neal, T. E. Mason, and J. E. Greedan (unpublished).